Partial Train Speed Trajectory Optimization Using Mixed-Integer Linear Programming

Article *in* IEEE Transactions on Intelligent Transportation Systems · March 2016

DOI: 10.1109/TITS.2016.2535399

CITATIONS
65

READS
653

5 authors, including:

Shaofeng Lu
South China University of Technology
105 PUBLICATIONS **1,632** CITATIONS
SEE PROFILE

Mingqiang Wang
Shandong University
45 PUBLICATIONS **2,131** CITATIONS
SEE PROFILE

Paul Weston
University of Birmingham
62 PUBLICATIONS **2,256** CITATIONS
SEE PROFILE

Chen Shuaixun
DNV KEMA Energy and Sustainability
28 PUBLICATIONS **2,392** CITATIONS
SEE PROFILE

Partial Train Speed Trajectory Optimization Using Mixed-Integer Linear Programming

Shaofeng Lu, *Member, IEEE*, Ming Qiang Wang, *Member, IEEE*,
Paul Weston, Shuaixun Chen, *Member, IEEE*, and Jie Yang

***Abstract*—The inexorable increase in energy demand around the world has put the energy-saving technology in hot spot for railway transportation. Train speed trajectory optimization based on optimal control, coasting control, and collaborative control inside railway systems is a popular methodology to enhance energy efficiency. This paper studies a special and interesting problem, i.e., the partial train speed trajectory optimization problem, and proposes a complete mathematical model where a mixed-integer linear programming algorithm can be directly applied. During the transient operation process of a train, the speed of the train is often considered to be monotonically increasing and decreasing in normal conditions without extreme gradients. Given that, the proposed method can quickly locate the train speed profile under practical engineering constraints, and the objective function is either to maximize the regenerative braking energy or to minimize the traction energy. Such a method with a short computational time may become particularly interesting for online cases where a train is altering its speed in a fixed distance and time due to the operational requirement. The generated speed trajectory can be used to guide the train to control its speed or in a normal braking operation. The robustness and effectiveness of the method has been demonstrated through a number of detailed simulation results in this paper.**

***Index Terms*—Mathematical modeling, energy efficiency, electric vehicle, regenerative braking energy.**

NOMENCLATURE

α	The instant gradient for the current position of the train.
Δd_i	The distance traveled when train reduce its speed from v_{i+1} to v_i
Δh_i	The height difference between h_i and h_{i+1}
Δt_i	The time that elapses when train reduce its speed from v_{i+1} to v_i
$\lambda_1, \lambda_2, \ldots, \lambda_5$	The special order set type 2 with 5 elements
A, B, and C	Davis coefficients
a_i^{tr}	The electric traction energy consumed when the train is accelerating from v_i to v_{i+1}
A_{brm}	The maximum allowed acceleration or deceleration rate.
D	The total braking distance
D_i	Distance information for the known locations.
d_i	The distance between the final position and the current position where the train is at a speed of v_i
d_i'	The distance interval between the location where the train is at a speed of v_i and the location where the train begins to brake
$d_{j,\mathrm{lim}}$	The distance between the speed limit switch point and the beginning position
E_i^{eb}	The regenerative braking energy in the distance interval Δd_i
F_i^{tr}	The electric traction effort imposed when the train is accelerating from v_i to v_{i+1}
F_{eb}	The instant electric braking effort
$F_{i,d}$	Average drag force between v_i and v_{i+1}
$F_{i,\mathrm{ebm}}$, $F_{i,\mathrm{etm}}$	The average maximum electric braking and traction effort between speeds v_i and v_{i+1}
H_i	Altitude information for the known locations
h_i	The current height at the position where the train is at a speed of v_i
i	Index of candidate speed
M	Mass of the train
M'	Effective mass of the train considering rotary effects
$T_{\min}$, $T_{\max}$	The minimum time and maximum time allowed for the entire acceleration and deceleration process.
v_i	Candidate speeds
$v_{i,\mathrm{avg}}$	Average speed between two adjacent speed candidates v_i and v_{i+1}
$v_{j,\mathrm{lim}}$	The speed limit level to the left of each speed limit switch point
$v_{\max}$	The maximum allowed operation speed of the train
N	Total number of candidate speeds
T	The fixed time allowed for the entire acceleration and deceleration process.

Manuscript received July 14, 2015; revised November 21, 2015 and December 31, 2015; accepted February 14, 2016. Date of publication March 14, 2016; date of current version September 30, 2016. This work was supported in part by the 2014 Jiangsu University Natural Science Research Program through Project 14KJB580010 and in part by the Research and Development Fund of Xi'an Jiaotong-Liverpool University through Project RDF-14-01-15. The Associate Editor for this paper was F.-Y. Wang.

S. Lu is with the Department of Electrical and Electronic Engineering, Xi'an Jiaotong-Liverpool University, Suzhou 215123, China (e-mail: Shaofeng.Lu@xjtlu.edu.cn).

M. Q. Wang is with the School of Electrical Engineering, Shandong University, Jinan 250061, China (e-mail: wang0367@hotmail.com).

P. Weston is with the School of Electronic, Electrical and Systems Engineering, University of Birmingham, Birmingham B15 2TT, U.K. (e-mail: p.weston@bham.ac.uk).

S. Chen is with Accenture, Singapore 179101 (e-mail: nosper@gmail.com).

J. Yang is with Beijing Jiaotong University, Beijing 100044, China, and also with Jiangxi University of Science and Technology, Ganzhou 341000, China (e-mail: 15405993@qq.com).

Color versions of one or more of the figures in this paper are available online at http://ieeexplore.ieee.org.

Digital Object Identifier 10.1109/TITS.2016.2535399

I. Introduction

With the inexorable increase of the energy demand and more emphasis being put on carbon emissions, railway transportation has been more concerned about the energy efficiency than ever [1]. Traction system plays a major role in moving the railway vehicle to satisfy customer service requirements and on the other hand, consumes a large proportion of the energy consumption for the railway transportation system. Improving the energy efficiency of the traction system brings significant impact on the total energy consumption of the railway transportation system [2].

The train speed trajectory optimization to reduce the energy consumptions has been the focus for a large number of research papers in the past few decades. Different methods have been proposed to find "the optimal train speed trajectory" with the minimum energy consumption or other costs. One of the commonly adopted techniques is to apply the designed coasting operation which uses up the allowable time and reduces the non-regenerative braking energy by varying the coasting margin. Due to the significance of coasting operation, during which the motors or engines are virtually shut down, a balance between the operation time and energy consumption can be optimized [3], [4]. Besides the coasting control, the general control using a variety of heuristic and numerical algorithms is also applied to locate the energy-efficient train trajectory [5]–[10]. By applying the Pontryagin Maximum Principle (PMP) in optimal control, global optimal solutions can be obtained given that certain conditions are met [11]–[15]. Discretization of the state space, in which each state contains the information of distance, speed, time and energy consumption etc., the dynamic programming and heuristic algorithms can be applied to obtain the discrete speed trajectory. However, the dynamic-programming-based methods suffer from the "curse of dimensionality" and state approximation due to discretization and has hardly found its application in online cases due to the heavy computational loads [6], [16]–[18]. In other papers, the train trajectory optimization problem is considered as one sub-problem in a two-level optimization problem for multitrain operations and timetable optimization [19]–[21].

On the other hand, as an important operation for electric railway vehicles, regenerative braking converts the kinetic energy into the reusable electric energy and improves the energy efficiency of the traction system [22]–[24]. Papers [25], [26] investigate the application of regenerative braking in electric railway systems. With the proper modeling, the regenerative braking energy (RBE) can be optimized together with the entire speed trajectory and achieve the optimal energy efficiency using PMP [12]. In order to improve the utilization of regenerative energy, some recent papers tries to improve the train scheduling to maximize the overlappings of train acceleration and braking phases within a railway network [27]–[30]. In particular, electric load flow calculation is considered in [30] and [31], putting on extra emphasis on electric network modeling and providing insights on the impact of electric network loss for regenerative braking energy recovery. Motivated by the unique characteristics of braking trajectory, some previous studies have been conducted on the partial train speed trajectory to maximize the regenerative braking energy (RBE) [17], [32]. Partial train speed trajectory optimization takes only one typical part of the entire speed trajectory as the optimization objective, e.g. the braking part, where the constraints can be linearized and thus simplified as demonstrated in [17] and [32]. The significance of the partial speed trajectory optimization to maximize the RBE can be found in the applications where the regenerative braking are commonly applied and limited space for improvement on other operation due to service constraints, and uncertainty of train operations [17].

Based on the previous work demonstrated in [17] and [32], this paper proposes a new mathematical model in which the Mixed Integer Linear Programming (MILP) can be applied. The speed series of the vehicle is assumed to be monotonously decreasing or increasing without losing its feasibility in practical applications and the speed trajectory is constrained within a fixed distance range and time window. Optimal solutions can be found for practical cases involving the engineering constraints such as the speed limits, route gradients and the characteristics of electrical motor. Especially, both electric braking and traction energy generated from the electric motors due to route gradients can be modeled and optimized simultaneously. It is worth mentioning that all these engineering constraints could be linearized based on the reasonable assumption of monotonicity of the speed series.

The advantage of the proposed method includes the robustness, flexibility and high computational efficiency. Compared to previous work [17], [32], the main contributions of this paper includes more complicated modeling involving gradients and accelerations to address issues arising from practical cases. The research outcomes can be easily extended to an intelligent transportation system or railway signaling system to facilitate the vehicle control systems and improve the energy efficiency.

This paper is organized as follows. Section II covers the MILP mathematical model where the non-linear speed limit and gradient constraints are included. Section III demonstrates case studies in various scenarios for the braking operations where RBE is to be maximized. Section IV discusses a case for acceleration operations where the electric motors provide the traction effort and the total traction energy is to be minimized. At the end, conclusions are drawn and future work of the research is discussed in Section VI.

II. Mathematical Modeling

During the braking procedure of a train, the braking effort can be provided by both electric and mechanical braking efforts. The mechanical braking is also commonly referred to as the "air" braking. A combination of braking efforts, the drag forces and forces due to gradients provide the total speed-reducing force to bring the speed of train to zero. In this paper, the total braking distance is considered as a known parameter while it actually varies from case to case. The train is required to arrive at the demanded position, i.e. the next train station within an allowed time window. The RBE can only be generated by the electric effort provided by the electric motor and for different train speed, the maximum electric braking effort will be different. A typical electric motor characteristics against the train speed, along with the changing drag forces due to air aerodynamic drag, rolling resistance and bearing drag against

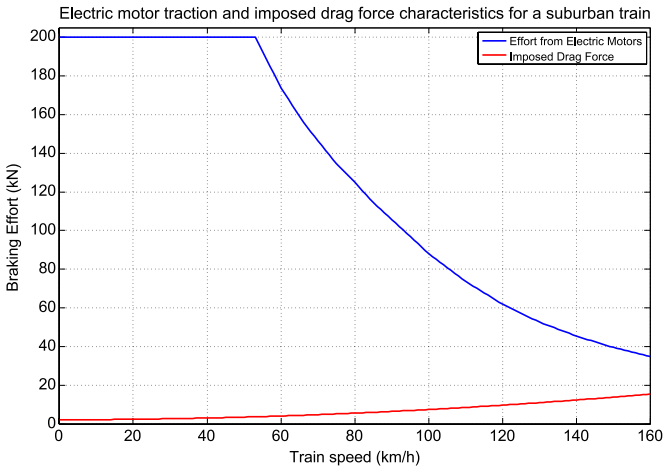

Fig. 1. Motor traction and imposed drag force characteristics for a typical suburban train.

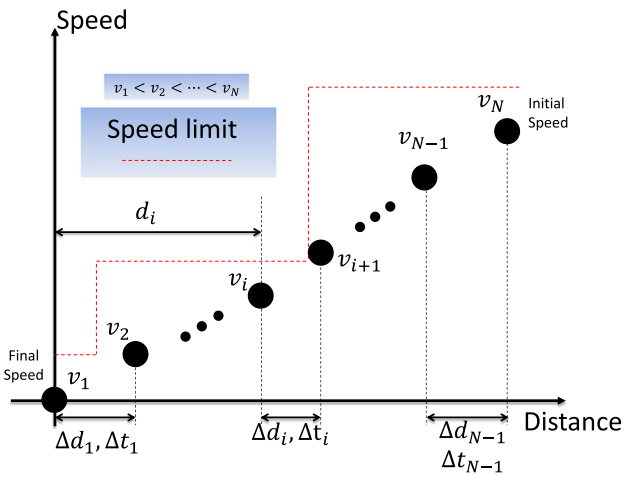

Fig. 2. Schematic of the MILP model for braking trajectory optimization.

the train speed is shown in Fig. 1. It is vastly different in terms of traction characteristics of electric motors during motoring and braking mode and the demonstration of this characteristics curve provides only a general relationship between the motor effort and the train speed.

The mathematical details of the MILP model are introduced as follows and the schematic demonstration is shown in Fig. 2.

It is assumed that there are series of monotonously increasing speeds along the braking trajectory, i.e. $v_1, v_2, \ldots, v_N$. and $v_1 < v_2 < \cdots < v_N$. For a typical braking trajectory where the train is demanded to stop at a set distance, $v_1 = 0$ is the final stop speed and v_N is the initial speed of the braking procedure. Note that the actual operation of the train begins from v_N and ends at v_1. However, in order to simplify the modeling, it is assumed the distance is increasing with the speed from v_1 to v_N while taking all the braking or drag forces as a positive force for this artificial "speed-up" process. This simplified modeling techniques will not affect its final optimization result.

In this paper, each speed is corresponding to the current train position. The distance between v_i and v_{i+1} means the distance between the positions where the train is at the speed of v_i and v_{i+1}. The total number of the speed N is set to sufficiently large to ensure that the average speed between two adjacent speeds will precisely reflect the current train speed and other conditions related to the train speed. If N is set and the initial speed v_N and final speed v_1 is known, the speed series is determined.

$$v_i = v_1 + (i-1)\frac{v_N - v_1}{N-1} \quad i = 1, 2, \ldots, N \tag{1}$$

The average speed $v_{i,avg}$ between v_i and v_{i+1} is calculated by (2):

$$v_{i,\text{avg}} = \frac{(v_i + v_{i+1})}{2} \quad i = 1, 2, \ldots, N-1 \tag{2}$$

The average drag force between v_i and v_{i+1} can be obtained by (3):

$$F_{i,d} = A + Bv_{i,\text{avg}} + Cv_{i,\text{avg}}^2 \quad i = 1, 2, \ldots, N-1 \tag{3}$$

where A, B, and C are the Davis coefficients.

The average maximum electric braking and traction effort between v_i and v_{i+1}, which is denoted by $F_{i,\text{ebm}}$ and $F_{i,\text{etm}}$ respectively, can be obtained by linearly interpolating the electric braking and traction characteristics. $F_{i,\text{ebm}} > 0$ and $F_{i,\text{etm}} < 0$. Refer to Fig. 1 for details. The consideration of real characteristics of regenerative braking operations can be easily incorporated as long as the characteristics are directly related to the speed of the train. For example, the regenerative braking effort can be set gradually decreasing to zero at lower speeds to model the inactiveness of regenerative braking during low speeds. In this paper, the electric braking and traction characteristics are regarded the same but nevertheless different characteristics can be easily adopted for both braking and traction in different cases.

The distance and time between v_i and v_{i+1} is denoted by Δd_i and Δt_i, where $i = 1, 2, 3, \ldots, N-1$. In the proposed model, Δd_i acts as the decision variable of the model. The relationship between Δd_i and Δt_i can be represented by (4)

$$\Delta t_i = \frac{\Delta d_i}{v_{\{i,\text{avg}\}}}. \tag{4}$$

Once Δd_i is determined, the entire solution for optimal braking trajectory is obtained. As shown in Fig. 2, d_i, is defined as the distance between the positions when the train is at a speed of v_0 and v_i and is calculated in (5). d_i will be used as the input to locate the information of the current height for the train at the speed of v_i, denoted by $h_{i,}$ using the piecewise linear relationship as shown in Fig. 4.

$$d_i = \sum_{n=1}^{i-1} \Delta d_n. \tag{5}$$

The total distance constraints should be met as shown in (6)

$$D = \sum_{i=1}^{N-1} \Delta d_i = d_{N-1}. \tag{6}$$

D is the total braking distance. The total time constraints should be met as listed in (7). Without loss of generality, the

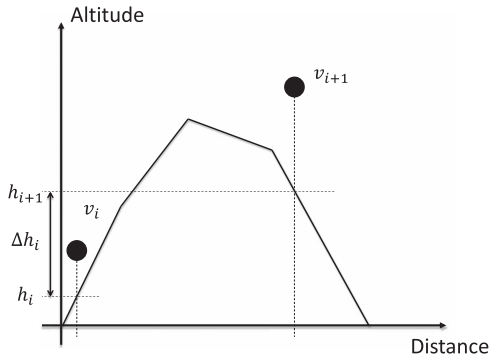

Fig. 3. Schematic demonstration for altitude information.

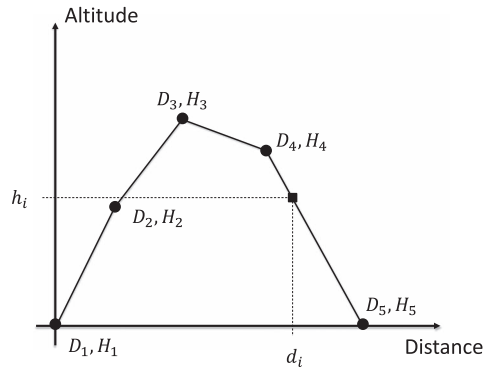

Fig. 4. A piecewise linear model for altitude information.

total time is constrained in a allowed time window as determined by $[T_{\min}, T_{\max}]$. In an extreme case, $T_{\min} = T_{\max} = T$, where T is the fixed journey time for the entire braking procedure.

$$T_{\min} \leq \sum_{i=1}^{N-1} \Delta t_i \leq T_{\max}. \tag{7}$$

The deceleration rate between v_i and v_{i+1} should not exceed the maximum braking rate defined by (8)

$$a_i^{\mathrm{br}} = \frac{v_{i+1}^2 - v_i^2}{2\Delta d_i} \leq A_{\mathrm{brm}}. \tag{8}$$

A_{brm} is a positively constant 1.2 m/s^2 in this study. Hence, it yields:

$$\Delta d_i \geq \frac{v_{i+1}^2 - v_i^2}{2A_{\mathrm{brm}}} \tag{9}$$

Thus, according to (4) and (9), it can be found that both Δt_i and Δd_i should be no less than zero. In order to incorporate the gradient information, we define Δh_i as the altitude difference between v_i and v_{i+1}. The schematic demonstration for d_i, Δh_i and h_i are shown in Fig. 3.

The maximum electric braking effort provided by the electric motors is limited by two factors: the electric motor characteristics and the maximum allowed total braking efforts. In other words, the electric effort provided from the motor should not exceed the maximum available electric effort and should not be too large so that the total braking efforts exceed the maximum allowed one. Two more constraints should be imposed in the model as shown in (10) and (11), where E_i^{eb} is the RBE generated in the distance interval Δd_i. M' and M are the effective mass and mass of the train respectively. In (11), it is demonstrated that the RBE can be negative to represent a traction operation with the presence of gradients and it is observed that RBE can be modeled in linear constraints including the altitude difference in each distance interval Δd_i

$$E_i^{\mathrm{eb}} \leq \left(M' a_i^{\mathrm{br}} - F_{i,d} + Mg\Delta h_i\right) \Delta d_i \tag{10}$$

$$-F_{i,\mathrm{etm}} \Delta d_i \leq E_i^{\mathrm{eb}} \leq F_{i,\mathrm{ebm}} \Delta d_i. \tag{11}$$

The relationship between d_i and h_i can be modeled using the piecewise linear (PWL) relationship. Due to the special discrete characteristics of altitude profile for route commonly adopted in railway modeling and simulation [3], [33], PWL is a well fit to locate the current altitude information for each speed.

An example with 5 altitude switch points is shown in Fig. 4. It is assumed that there are 5 known locations with distance D_i and altitude H_i and altitude information can obtained using the linear interpolation. We also assume that $D_1 = 0$ and $D_5 = D$, so that all the interpolated points are between D_1 and D_5. Note that the number of altitude switch point can be varied according to the constraint of the case scenario.

The following mixed-integer constraints should be imposed on the MILP model:

$$\lambda_1 + \lambda_2 + \cdots + \lambda_5 = 1 \tag{12}$$

$$\lambda_i \geq 0 \quad i = 1, 2, \ldots, 5 \tag{13}$$

$$\lambda_1 D_1 + \lambda_2 D_2 \ldots + \lambda_5 D_5 = d_i \tag{14}$$

$$\lambda_1 H_1 + \lambda_2 H_2 + \cdots + \lambda_5 H_5 = h_i \tag{15}$$

where $\lambda_1, \lambda_2, \ldots, \lambda_5$ are the special order set type 2 (SOS2) and they are non-negative real numbers as defined by (13) [34], $D_1, D_2, \ldots D_5$ are the 5 known distances and $H_1, H_2, \ldots, H_5$ are the 5 corresponding altitudes for each switch point in the example as shown in Fig. 4. The number of known points can vary from case to case.

By definition, no more than two non-zeros can be found for $\lambda_1, \lambda_2, \ldots, \lambda_5$. SOS2 speeds up the search procedure in branch and bound algorithm. Although members of SOS2 are continuous, the model containing SOS2 itself remains discrete and requires a mixed integer optimizer for the solution [35]. This ensures that a PWL relationship between d_i and h_i can be established. Considering the linear relationship between d_i and the input variable Δd_i, the altitude information can be incorporated as a PWL form in the model.

Speed limits are commonly applied via signals in railway systems. During the braking procedure, the train should keep its speed under the limit at all times. This constraint can be modeled using a linear inequality given the speed candidates are monotonous. One example is shown in Fig. 5. First, a speed limit switch point (SLSP) is defined as the location where the speed limit is changed. Second, we obtain the speed limit $v_{j,\mathrm{lim}}$ as shown in Fig. 5. Third, we locate the distance interval between the SLSP and the initial position of the braking

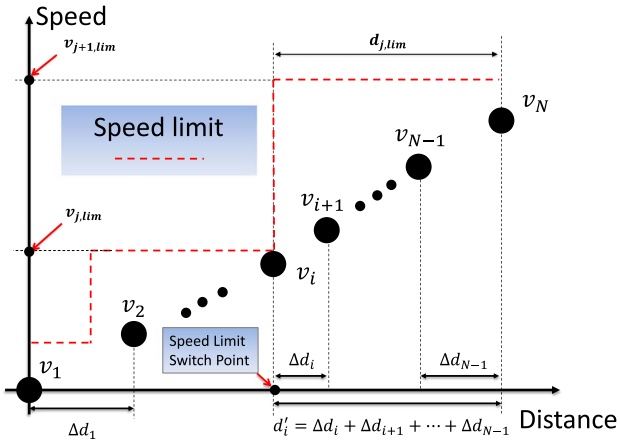

Fig. 5. Speed limit considerations for MILP model.

procedure, denoted by $d_{j,\lim}$. Fourth, the speed v_i in the speed series is achieved and $v_i = v_{j,\lim}$.[1] We define another distance variable d'_i as follows:

$$d'_i = \Delta d_i + \Delta d_{i+1} + \cdots + \Delta d_{N-1}. \tag{16}$$

In order to ensure all train speeds to be less than $v_{j,\lim}$, when the train goes across the SLSP, the following constraint should be met. This ensures that all the speeds higher than $v_{j,\lim}$ will not reach the controlled sections by $v_{j,\lim}$ and thus the speed constraints will be met if all this constraints are imposed for each speed limit

$$d_{j,\lim} \geq d'_i. \tag{17}$$

To summarize, the entire MILP model has been introduced in this section. Using the distance interval section Δd_i as the input variables of the optimization objective function, the optimization objective function can be presented by (18). Note that E_i^{eb} is a piecewise linear function of the decision variable Δd_i which is a positive real number

$$\begin{aligned} &\max_{\Delta d_i} \quad \sum_{i=1}^{N-1} E_i^{\text{eb}}(\Delta d_i) \\ &\text{s.t.} \quad (1)-(17) \\ &\Delta d_i \in \mathbb{R}. \end{aligned} \tag{18}$$

Once the optimization has been completed, the actual force distributions based on the optimization process can be calculated using a post-calculation process. In each distance interval, the train is assumed to go through a constant-acceleration process with very little changes on the initial speed and final speed. (19) is used to recover the actual electric braking effort.

$$F_{\text{eb}} = \max\left(M' a_i^{\text{br}} - F_{i,d} - Mg(\sin\alpha),\ F_{i,\text{ebm}}\right) \tag{19}$$

where "max" is the maximization function to choose any larger value between the two inputs; α is the instant gradient for the current position of the train. α is negative if the force due to gravity is a providing negative force against the motion of the train. The gradient may vary over a distance interval of Δd_i. This may cause a sudden change of the braking force but will not affect the optimization results. This is because the optimization is dealing with the potential energy between two adjacent positions and the changing gradients in between has a constant potential energy. F_{eb} is the instant electric braking effort for the current position of the train. (19) ensures that the braking energy will always be maximized once the optimization algorithm has determined the results. A good agreement has been found between the direct optimization results and the post calculation processes.

[1]We assume that N is sufficiently large so that the speed limit $v_{j,\lim}$ can be equal to one of the candidate speeds v_i if $v_{j,\lim} \in [v_1, v_N]$. For the cases where $v_{j,\lim} \notin [v_1, v_N]$ the constraints will be automatically relaxed.

TABLE I
MODELING PARAMETERS FOR A TYPICAL SUBURBAN VEHICLE

$M(t)$	$M'(t)$	$v_{max}(m/s)$	A	B	C
170	178	44.4	2.0895	0.0098	0.0065

TABLE II
OPTIMIZATION CONSTRAINT PARAMETERS AND RESULTS IN A SIMPLE CASE SCENARIO

Case	v_N (m/s)	T_{max} (s)	RBE (kWh)	Initial kinetic energy (kWh)	Recover rate(%)
1	44.4	∞	38.06	46.55	81.8
2	35	∞	27.86	28.92	96.3
3	35	70	26.38	28.92	91.2

III. CASES FOR BRAKING OPERATIONS

A. Simple Cases

In [17], a simple case scenario is discussed where the train is braking on a level track without considering the speed limit, the route gradients and total braking time limits. In this simple case, the train can only apply the braking effort but not the traction effort causing the lower bound of E_i^{eb} to be constrained by zero value. It is concluded that an optimal braking operation where the maximum RBE can be achieved may include three operations. They are the full-braking operation with both maximum electric braking and mechanical braking effort applied, the full-electric-braking operation with maximum electric braking effort applied and the coasting operation with only drag force applied. Usually the maximum-braking-rate constraint should be imposed in the full-braking operation. The sequence of these three operations will remain unchanged while these operations may not exist at the same time. If applied, the full-electric-braking operation will come after the full braking operation and the coasting will come after the full-electric-braking operation.

In this section, a simple case study without considering the speed limits and gradients has been conducted. The vehicle parameters for a typical suburban train are shown in Table I.

Three cases have been conducted. The optimization constraints and results are summarized in Table II. The recovery rate is the ratio of recovered RBE to the initial kinetic energy of the train.

Using (19), the effort distribution can be also calculated. The gradients information is ignored and the recovered effort

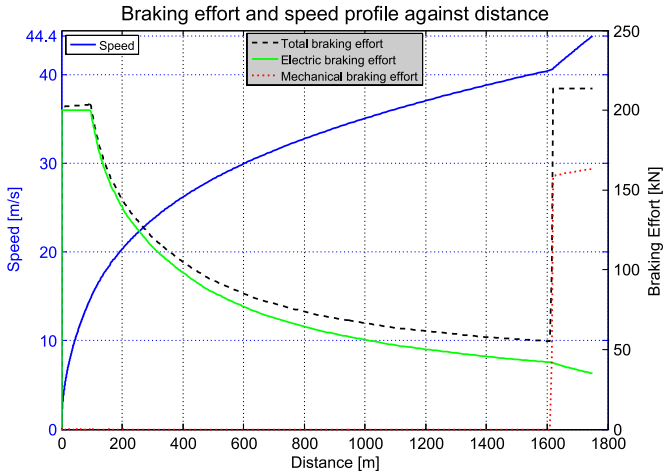

Fig. 6. Speed trajectory and braking efforts distribution for case 1.

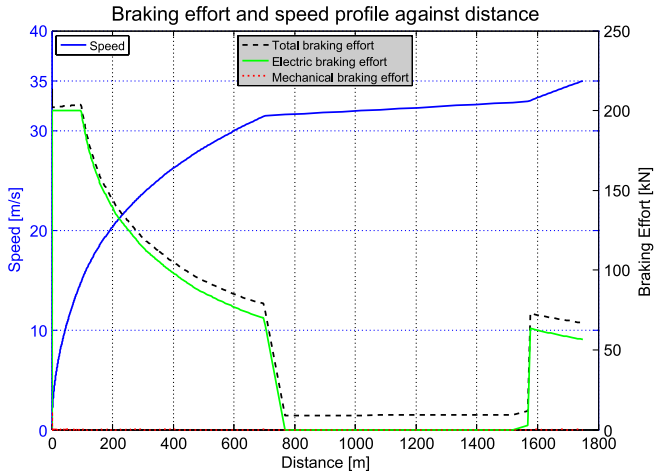

Fig. 8. Speed trajectory and braking efforts distribution for case 3.

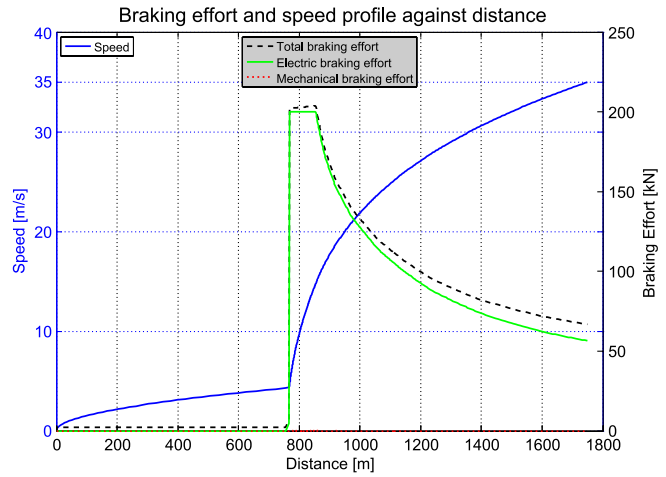

Fig. 7. Speed trajectory and braking efforts distribution for case 2.

complete agrees with the speed trajectory obtained in optimization results. The optimization results with the braking speed trajectory and the braking effort distribution are shown in Figs. 6–8.

It is observed that the conclusions based on the optimal control analysis agrees with the simulation results as shown in case 1 and case 2 where no braking-time constraint is imposed. In case 1, the initial speed is 44.4 m/s and the mechanical braking effort should be imposed at the beginning of the journey. The optimization algorithm will determine when the mechanical braking effort should be removed from the braking procedure.

In case 2, when the initial braking speed is reduced from 44.4 m/s to 35 m/s, no mechanical braking effort is needed in the entire braking procedure and the coasting operation will occur at the end of the braking procedure. The train speed is usually reduced to a lower level to reduce the impact of the drag force. In case 3, the time limit constraint is applied based on the constraints of case 2, the operations include both full-electric braking and coasting braking. Due to the time constraint, the coasting operation is applied when the train is at a high speed and the sequence of operations will by large rely on the constraints of various case scenarios.

TABLE III
OPTIMIZATION PARAMETERS AND RESULTS FOR PRACTICAL ENGINEERING SCENARIOS

Case	v_N (m/s)	T_{max} (s)	RBE (kWh)	Initial kinetic energy (kWh)	Potential energy (kWh)
4	35	130	-2.08	28.92	-13.9
5	35	130	38.28	28.92	13.9
6	44	80.65	35.51	45.71	13.9
7	44	∞	53.66	45.71	13.9

B. Cases With Speed Limits and Gradient Constraints

This section continues with a study on partial trajectory optimization for the braking procedure. In this study, practical engineering constraints including the speed limits and gradients are taken into account in optimization. The assumption for the braking procedure remains the same, i.e. the speed of train will be monotonous. Due to the impact of the gradients, the electric braking effort may not necessarily be positive and will not remain constant within a distance interval Δd_i. Similarly, (19) is applied to recover the effort distribution during the braking procedure.

Table III lists the optimization parameters and results for cases in practical engineering scenarios. In order to demonstrate the impact of gradients, the relative potential energy is calculated using: $Mg\Delta h_a$, where Δh_a is the altitude difference between the initial position and final position. A negative potential energy demonstrates a uphill trend between the initial braking position and the final arrival position as in Case 4.

Case 4 and case 5 are the two cases with reverse gradients. With the optimization results shown in Figs. 9 and 10, case 4 is dealing with a route with a downhill gradient first and change to a uphill one. Case 5 is taking a route with a gradient the other way round and its optimization results are shown in Figs. 11 and 12.

In both cases, mechanical braking efforts are applied at the beginning of the braking procedure to ensure that the speed limit reduction at the position of 1500 m can be met. But mechanical braking efforts have been kept at a minimum level throughout the braking procedure. As long as the electric braking effort could meet the braking effort demand, the mechanical

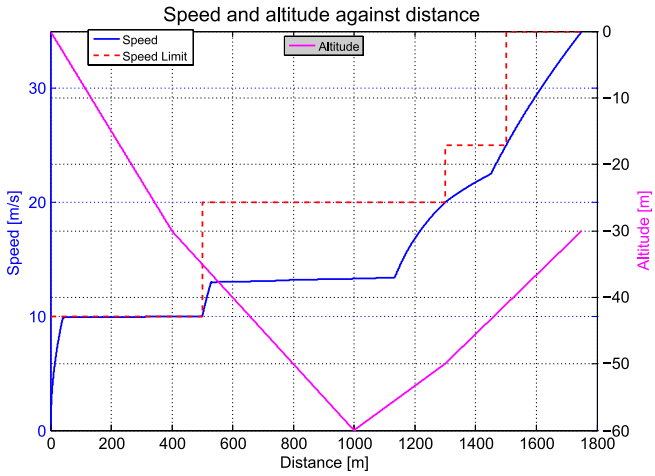

Fig. 9. Speed trajectory and altitude profile for case 4.

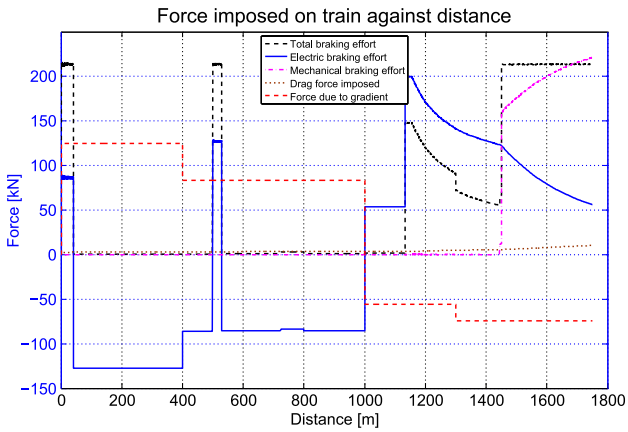

Fig. 10. Forces imposed on the train during braking procedure for case 4.

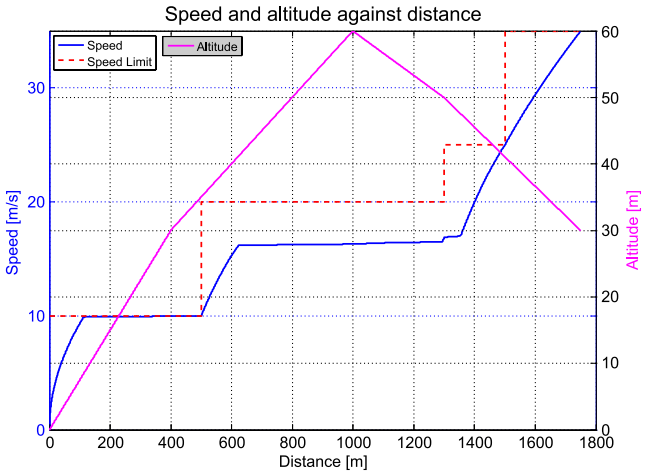

Fig. 11. Speed trajectory and altitude profile for case 5.

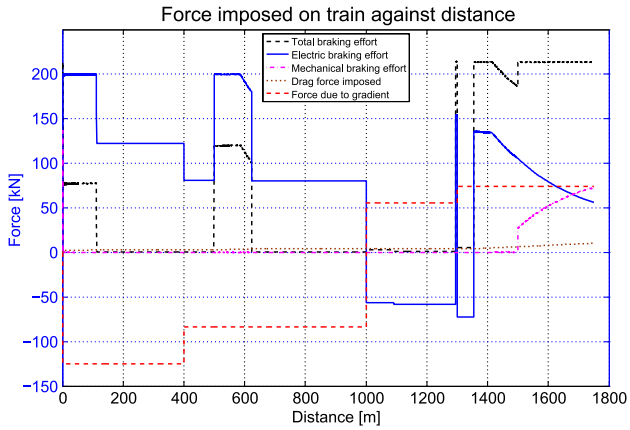

Fig. 12. Forces imposed on the train during the braking procedure for case 5.

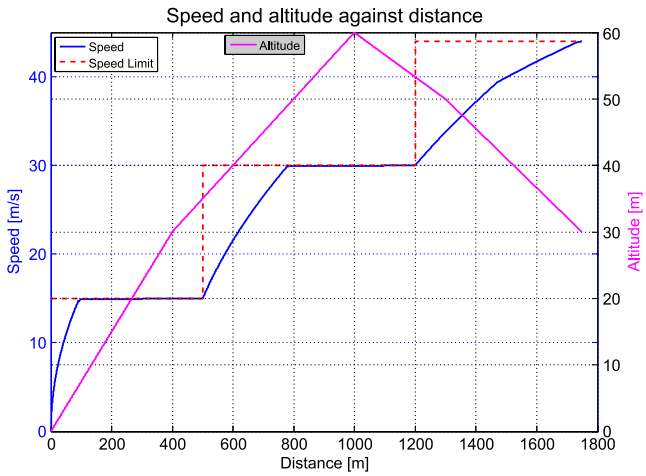

Fig. 13. Speed trajectory and altitude profile for case 6.

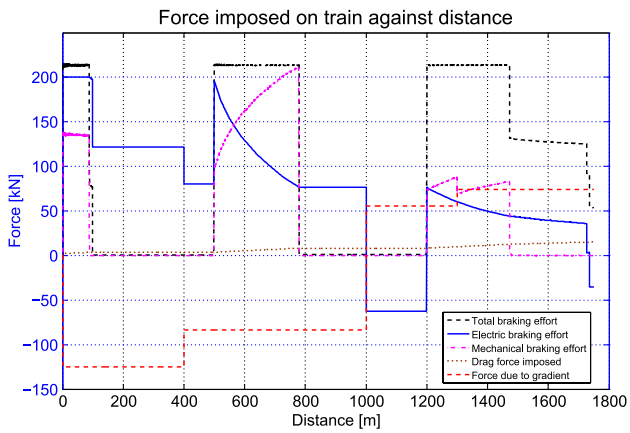

Fig. 14. Forces imposed on the train during the braking procedure for case 6.

braking effort will be prevented from using. It is also observed that the gradient change takes a major impact on the operations of the electric motors. In the uphill sections, the electric motors turn into the traction mode providing negative braking efforts.

Case 6 is an extreme case with a close-to-shortest braking time, i.e. 80.65 s. The optimization results are shown in Figs. 13 and 14. The gradient constraint is the same as case 5. It is observed that the braking trajectory is taking the maximum braking effort during speed changing due to speed limits or the arrival requirement and keeping a minimum change close to the speed limits. Since the speed changes insignificantly over a long distance with a very low deceleration rate, this part of operation can be regarded as the psudo-cruising operation.

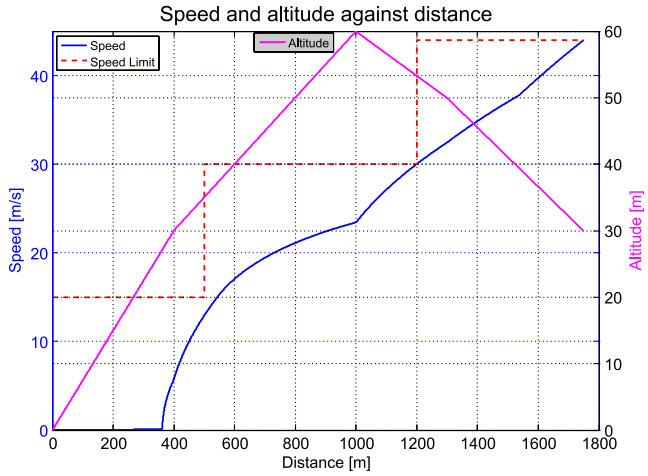

Fig. 15. Speed trajectory and altitude profile for case 7.

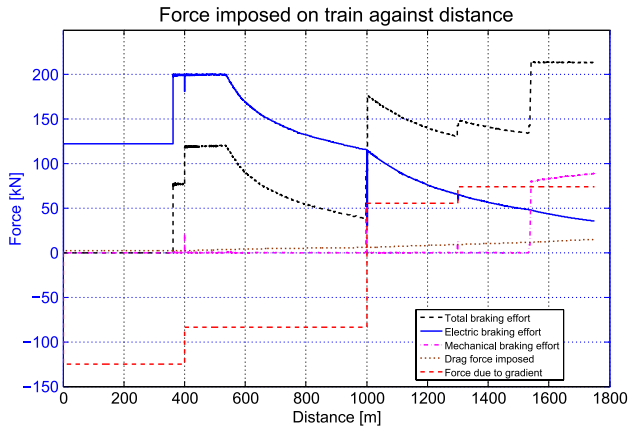

Fig. 16. Forces imposed on the train during the braking procedure for case 7.

In this case, gradients are found to have certain impacts on the braking procedure. For instance, for the psudo-cruising operation, traction effort should be imposed between 1000 m and 1200 m while regenerative braking efforts are required for the section between 800 m and 1000 m.

Case 7, as illustrated by Figs. 15 and 16, demonstrates another extreme case scenario with no maximum braking time requirement by setting the maximum braking time to infinity. It is seen that the train speed is reduced to a very small value before reaching the final stop point. Lower speed reduces the impact of the drag forces imposed on the train. But it is also noted that the speed-reduction process is mostly done by electric-braking efforts while the mechanic braking efforts are only imposed at the beginning of the braking process. The mechanical braking efforts remain nearly zero until the end of the journey. At the final session of the braking operation between distance of 0 m and 362 m, the electric braking effort is mainly applied to counteract with the forces due to gradients and drag forces. The total deceleration rate is close to zero leading to a psudo-cruising operation.

Table IV summarizes the information about the optimization models and the computational time for each case. The information is obtained based on a desktop computer installed with Intel i5-3470 @ 3.20 GHz CPU and 4.00 GB RAM.

TABLE IV
A SUMMARY OF MIXED INTEGER MODEL INFORMATION AND COMPUTATIONAL TIME FOR CASES 1–7

Case No.	No. of real variables	No. of SOS2 variables	No. of Constraints	Computation time (s)
1	1332	0	1778	0.02
2	1050	0	1402	0.05
3	1050	0	1402	0.03
4	3858	351	3160	13.13
5	3858	351	3160	9.06
6	4848	441	3969	9.70
7	4848	441	3969	13.41

IV. A CASE FOR ACCELERATING OPERATIONS

In Section III, the braking effort is modeled as a positive effort and the traction effort is modeled as a negative effort. The objective function is to be maximized since more energy to be resulted by the electric braking effort, more RBE will be recovered. A similar model can be applied for the acceleration case where the speed of the train is considered monotonously increasing. There are no steep gradients on the route so that the monotonous speed series can be maintained by the electric motors only. There are no air braking and only electric "braking" will be applied. In practical application, this "braking" effort is actually the traction effort to speed up the train. The objective function is to be minimized to reduce the energy done by the electric traction effort. Compared to the mathematical model introduced in Section II, a few modifications should be done in the mathematical modeling as previously introduced in Section II.

First, (8) is no longer needed since the maximum acceleration rate will be determined by the traction motors.

Second, (10) and (11) should be changed into (20) and (21) respectively. E_i^{et} is the electric traction energy applied during acceleration procedure and a_i^{tr} is the acceleration rate between v_i and v_{i+1} as defined by (22).

Third, the traction effort F_i^{tr} can be recovered after E_i^{et} and Δd_i are obtained

$$E_i^{\mathrm{et}} = \left(M' a_i^{\mathrm{tr}} + F_{i,d} + Mg\Delta h_i\right)\Delta d_i \tag{20}$$

$$-F_{i,\mathrm{ebm}}\Delta d_i \le E_i^{\mathrm{et}} \le F_{i,\mathrm{etm}}\Delta d_i \tag{21}$$

$$a_i^{\mathrm{tr}} = \frac{v_{i+1}^2 - v_i^2}{2\Delta d_i}. \tag{22}$$

Finally, the objective function shown in (18) will be changed into (23) subject to constraints

$$\min_{\Delta d_i} \sum_{i=1}^{N-1} E_i^{\mathrm{eb}}(\Delta d_i). \tag{23}$$

A simulation study has been set up for a train to accelerate from zero speed to 35 m/s for a distance of 1750 m and a time of 100 s. Fig. 17 shows the speed and altitude against distance during the acceleration process. The train is set off from distance 0 m to 1750 m and going uphill for the first 1000 m and downhill for the rest of 750 m. The electric motor as the only traction effort source corresponds well with the change of the gradient. As shown in Fig. 18, the electric effort turns from positive to negative to respond to a sudden change of gradient at 1000 m. Due to the total journey time constraint, the proposed

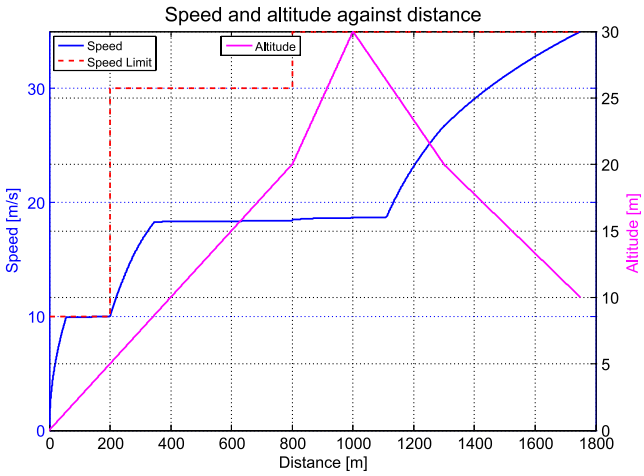

Fig. 17. Speed and altitude information for an acceleration operation.

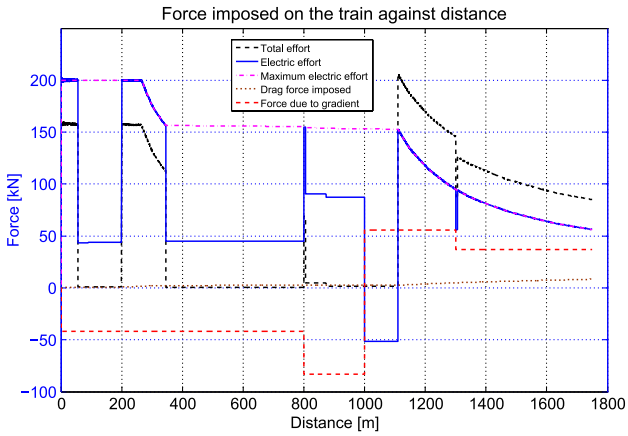

Fig. 18. Forces imposed on the train during an acceleration operation.

algorithm is able to locate the speed level of pseudo-cruising operation between the distance of 280 m and 1100 m.

The final traction energy consumption of the optimized trajectory is 36.57 kWh and the braking energy is assumed to be fully recovered to counteract the traction energy. The final train kinetic energy is 21.25 kWh and increment of potential energy is 4.63 kWh with 10.68 kWh consumed by the drag forces.

V. Discussion on the Model

The monotonicity of train speeds in the proposed model is the fundamental assumption in this paper. The rationality of this assumption lies on observations from urban rail transportation systems where the train is required to be powerful enough to readily increase and decrease the speed during the journey. It is usually undesirable to increase the speed during a braking procedure or decrease the speed during an acceleration procedure. The proposed model tries to tackle a special but common problem in railway engineering using a numerical optimization technique. Preliminary results shown in [17] has demonstrated an agreement between the optimization result and the analysis based on optimal control theory.

Given the monotonicity of train speeds, the speed-holding, coasting, braking and motoring operations can be approximated by giving a sufficiently small difference between two adjacent speed candidates. However, the fundamental assumption imposes limitations and constraints on the proposed model for its potential application. It is out of the scope of this paper to deal with more general cases where the monotonicity of train speeds becomes impossible due to extremities of gradient or other factors.

VI. Conclusion

Different from previous research on train trajectory optimization, this paper studied a special problem, i.e. the partial train speed trajectory optimization problem based on MILP. Given that the candidate speeds of the train are monotonous and the total journey length is determined, the speed trajectory can be optimized either by maximizing the RBE or by minimizing the traction energy consumption. A number of case studies have been discussed to evaluate the robustness and effectiveness of the proposed method. The proposed method is able to quickly locate the partial train speed trajectory for online applications. In a simple case without the changing gradient information, the calculation time is on a scale of millisecond and the calculation remains in a scale of seconds for cases with the changing gradients constraints.

With regard to the future work, the current study needs to consider applying the proposed method in more practical railway scenarios with the practical characteristics of braking systems and railway signal systems. The current study only considers electric motors and generators with an energy efficiency of 100% and ignores the practical characteristics of regenerative braking and mechanical braking operations. For example, the air braking may not be ready at the initial stage of braking since it takes time to increase the pressure of the compressed air for the entire braking system. The electric braking characteristics can be much different from the one as shown in our current research. The monotonicity of the candidate speeds cannot be guaranteed if extreme gradients exist along the route and this sets its application preference to urban railway or high-speed railway systems where extreme gradients are found much unusual. But nevertheless the optimization method proposed in this paper can be further applied in railway control and operations and can be further extended to a wider range of intelligent transportation systems.

References

[1] "UIC and IEA Railway Handbook 2014—Energy Consumption and co2 Emissions," Int. Union Railways (IUR), Paris, France, 2014.

[2] A. González-Gil, R. Palacin, P. Batty, and J. P. Powell, "A systems approach to reduce urban rail energy consumption," *Energy Convers. Manage.*, vol. 80, pp. 509–524, 2014.

[3] Y. V. Bocharnikov, A. M. Tobias, C. Roberts, S. Hillmansen, and C. J. Goodman, "Optimal driving strategy for traction energy saving on dc suburban railways," *Electric Power Appl., IET*, vol. 1, no. 5, pp. 675–682, 2007.

[4] Y. Ding, H. Liu, Y. Bai, and F. Zhou, "A two-level optimization model and algorithm for energy-efficient urban train operation," *J. Transp. Syst. Eng. Inf. Technol.*, vol. 11, no. 1, pp. 96–101, 2011.

[5] B.-R. Ke, C.-L. Lin, and C.-W. Lai, "Optimization of train-speed trajectory and control for mass rapid transit systems," *Control Eng. Pract.*, vol. 19, no. 7, pp. 675–687, 2013.

[6] B.-R. Ke, C.-L. Lin, and C.-C. Yang, "Optimisation of train energy-efficient operation for mass rapid transit systems," *Intell. Transp. Syst., IET*, vol. 6, no. 1, pp. 58–66, 2012.

[7] B.-R. Ke, M.-C. Chen, and C.-L. Lin, "Block-layout design using max-min ant system for saving energy on mass rapid transit systems," *IEEE Trans. Intell. Transp. Syst.*, vol. 10, no. 2, pp. 226–235, Jun. 2009.
[8] M.-H. Kang, "A GA-based algorithm for creating an energy-optimum train speed trajectory," *J. Int. Council Elect. Eng.*, vol. 1, no. 2, pp. 123–128, 2011.
[9] Y. Wang, B. De Schutter, B. Ning, N. Groot, and T. J. van den Boom, "Optimal trajectory planning for trains using mixed integer linear programming," in *Proc. IEEE 14th Int. ITSC*, 2011, pp. 1598–1604.
[10] Y. Wang, B. Ning, F. Cao, B. De Schutter, and T. J. van den Boom, "A survey on optimal trajectory planning for train operations," in *Proc. IEEE Int. Conf. SOLI*, 2011, pp. 589–594.
[11] A. R. Albrecht, P. G. Howlett, P. J. Pudney, and X. Vu, "Energy-efficiency train control: From local convexity to global optimization and uniqueness," *Automatica*, vol. 49, pp. 3072–3078, 2013.
[12] E. Khmelnitsky, "On an optimal control problem of train operation," *IEEE Trans. Autom. Control*, vol. 45, no. 7, pp. 1257–1266, Jul. 2000.
[13] P. Howlett, P. J. Pudney, and X. Vu, "Local energy minimization in optimal train control," *Automatica*, vol. 45, no. 11, pp. 2692–2698, 2009.
[14] P. Howlett, "The optimal control of a train," *Ann. Oper. Res.*, vol. 98, pp. 65–87, 2000.
[15] R. Liu and I. M. Golovitcher, "Energy-efficient operation of rail vehicles," *Transp. Res. A, Policy Pract.*, vol. 37, no. 10, pp. 917–932, 2003.
[16] S. Lu, S. Hillmansen, T. K. Ho, and C. Roberts, "Single-train trajectory optimization," *IEEE Trans. Intell. Transp. Syst.*, vol. 14, no. 2, pp. 743–750, Jun. 2013.
[17] S. Lu, P. Weston, S. Hillmansen, H. B. Gooi, and C. Roberts, "Increasing the regenerative braking energy for railway vehicles," *IEEE Trans. Intell. Transp. Syst.*, vol. 15, no. 6, pp. 2506–2515, Dec. 2014.
[18] S. Lu, "Optimising Power Management Strategies for Railway Traction Systems," Ph.D. dissertation, School Electron., Elect. Comput. Eng., Univ. Birmingham, Birmingham, U.K., 2011.
[19] S. Su, T. Tang, X. Li, and Z. Gao, "Optimization of multitrain operations in a subway system," *IEEE Trans. Intell. Transp. Syst.*, vol. 15, no. 2, pp. 673–685, Apr. 2014.
[20] S. Su, X. Li, T. Tang, and Z. Gao, "A subway train timetable optimization approach based on energy-efficient operation strategy," *IEEE Trans. Intell. Transp. Syst.*, vol. 14, no. 2, pp. 883–893, Jun. 2013.
[21] X. Li, C.-F. Chien, L. Li, Z. Gao, and L. Yang, "Energy-constraint operation strategy for high-speed railway," *Int. J. Innovative Comput., Inf. Control*, vol. 8, no. 10(A), pp. 6569–6583, 2012.
[22] A. González-Gil, R. Palacin, and P. Batty, "Sustainable urban rail systems: Strategies and technologies for optimal management of regenerative braking energy," *Energy Convers. Manage.*, vol. 75, pp. 374–388, 2013.
[23] K. Kondo, "Recent energy saving technologies on railway traction systems," *IEEJ Trans. Elect. Electron. Eng.*, vol. 5, no. 3, pp. 298–303, May 2010.
[24] V. Gelman, "Braking energy recuperation," *IEEE Veh. Technol. Mag.*, vol. 4, no. 3, pp. 82–89, Sep. 2009.
[25] M. Shafighy, S. Khoo, and A. Z. Kouzani, "Modelling and simulation of regeneration in ac traction propulsion system of electrified railway," *IET Elect. Syst. Transp.*, vol. 5, no. 4, pp. 145–155, Dec. 2015.
[26] S. de la Torre, A. J. Sanchez-Racero, J. A. Aguado, M. Reyes, and O. Martianez, "Optimal sizing of energy storage for regenerative braking in electric railway systems," *IEEE Trans. Power Syst.*, vol. 30, no. 3, pp. 1492–1500, May 2015.
[27] X. Li and H. K. Lo, "Energy minimization in dynamic train scheduling and control for metro rail operations," *Transp. Res. B*, vol. 70, pp. 269–284, 2014.
[28] X. Yang, A. Chen, X. Li, B. Ning, and T. Tang, "An energy-efficient scheduling approach to improve the utilization of regenerative energy for metro systems," *Transp. Res. C*, vol. 57, pp. 13–29, 2015.
[29] S. D. Gupta, L. Pavel, and J. K. Tobin, "An optimization model to utilize regenerative braking energy in a railway network," in *Proc. ACC*, 2015, pp. 5919–5924.
[30] M. Peña Alcaraz, A. Fernández, A. P. Cucala, A. Ramos, and R. R. Pecharromán, "Optimal underground timetable design based on power flow for maximizing the use of regenerative-braking energy," *Proc. Inst. Mech. Eng., F, J. Rail Rapid Transit*, vol. 226, no.4, pp. 397–408, 2012.
[31] Z. Tian *et al.*, "Energy evaluation of the power network of a dc railway system with regenerating trains," *IET Elect. Syst. Transp.*, Oct. 2015. [Online.] Available: http://digital-library.theiet.org/content/journals/10.1049/iet-est.2015.0025
[32] S. Lu, P. Weston, and N. Zhao, "Maximise the regenerative braking energy using linear programming," in *Proc. IEEE 17th ITSC*, 2014, pp. 2499–2504.
[33] S. Lu, S. Hillmansen, and C. Roberts, "A power management strategy for multiple unit railroad vehicles," *IEEE Trans. Veh. Technol.*, vol. 60, no. 2, pp. 406–420, Feb. 2011.
[34] IBM, IBM ILOG CPLEX V12.1-User's Manual for CPLEX, 2009.
[35] E. Beale and J. H. Forrest, "Global optimization using special ordered sets," *Math. Program.*, vol. 10, no. 1, pp. 52–69, 1976.

Shaofeng Lu received the B.Eng. degree from Huazhong University of Science and Technology, Wuhan, China, and the B.Eng. and Ph.D. degrees from the University of Birmingham, Birmingham, U.K., in 2007 and 2011, respectively, all in electrical and electronic engineering. He is a Lecturer with the Department of Electronic and Electrical Engineering, Xi'an Jiaotong-Liverpool University, Suzhou, China. His main research interests include power management strategies, railway traction system modeling, optimization technique application, and energy-efficient transportation systems.

Ming Qiang Wang (S'08–M'12) received the Ph.D. degree from Nanyang Technological University, Singapore, in 2012.

He is currently a Lecturer with the School of Electrical Engineering, Shandong University, Jinan, China. His research interests include power system economic operation and microgrids.

Paul Weston received the B.Eng. degree in electronics and control engineering in Birmingham in 1992 and the Ph.D. degree in nonlinear system identification in Birmingham in 1999. Since 2002, he has been a Research Fellow with the Railway Research Group of the University of Birmingham, working on electronics hardware, firmware, software, and signal processing algorithms. His current research interests include railway vehicle energy instrumentation and modeling, railway asset condition monitoring, instrumentation, and signal processing.

Shuaixun Chen (M'13) received the B.S. degree in power engineering and business administration from Wuhan University, Wuhan, China, in 2007 and the M.Sc. and Ph.D. degrees in power engineering from Nanyang Technological University (NTU), Singapore, in 2008 and 2012, respectively. From 2012 to 2013, he was a Research Fellow with the Energy Research Institute, NTU. From 2013 to 2015, he was a Microgrid/Smart Grid Consultant with DNV GL Energy (formerly KEMA). He is currently with Accenture Singapore. Throughout his career, he has developed expertise in smart energy management systems, energy efficiency, renewable energy sources and energy storage systems, and power system operation and planning.

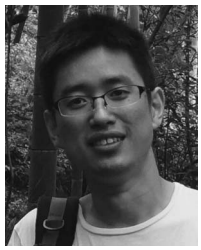

Jie Yang was born in Anhui, China, in 1979. He received the B.Sc. degree in electrical engineering and the M.Sc. degree in control theory and control engineering from Jiangxi University of Science and Technology, Ganzhou, China, in 2002 and 2005, respectively. He is currently working toward the Ph.D. degree in the State Key Laboratory of Rail Traffic Control and Safety, Beijing Jiaotong University, Beijing, China.

In 2005, he joined Jiangxi University of Science and Technology, where he has been an Associate Professor with the School of Electrical Engineering and Automation since 2012. His current research interests mainly focus on energy-efficient train control and its applications.